Earthquake Engineering, Tenth World Conference © 1992 Balkema, Rotterdam. ISBN 90 5410 060 5

Substructured hybrid loading tests of steel box-section columns for inelastic earthquake response of frame structures

Yoshikazu Yamada & Hirokazu Iemura
Department of Civil Engineering, Kyoto University, Japan

William Tanzo
Department of Construction Engineering, Saitama University, Japan

ABSTRACT: Inelastic earthquake response and cyclic behavior of steel box-shaped piers under combined axial, shear, and bending loads are presented. For this purpose, a three degree-of-freedom loading and control system has been developed. First, cyclic loading tests were conducted on the steel column specimens in which patterns of combined axial, shear, and bending loads were imposed. In the second part of the testing program, inelastic earthquake response of two-story structural steel frames was determined by substructured hybrid loading tests. The first-story columns were taken as the experimental substructures, while the rest of the structure was modeled by analytical substructures. The main objective is to investigate the inelastic behavior of steel box-section columns of a frame structure under earthquake ground motions. Girder stiffness has a large effect on the failure mode and behavior of columns. Most importantly, the consequent behavior of the columns greatly affects the overall response of the total structure.

1 INTRODUCTION

Understanding of inelastic nonlinear behavior of members and total structures is a key to estimate safety of steel structures against possible strong earthquake ground motion. Recent observation of earthquake motion has suggested high possibility of structural response exceeding the yielding limits especially for high-rise or long-span structures. Hence, it is becoming critically important to investigate earthquake safety of these structures in the inelastic range.

In earthquake-resistant design of steel frame structures, it is of importance to ensure that the columns are provided with adequate ductility and energy-dissipation capacity to survive severe earthquakes. Extensive experimental tests are needed to study this complex behavior. Conventionally, experimental studies have been conducted on specimens by quasi-static cyclic loading tests using arbitrarily prescribed loading histories. However, results from quasi-staic tests do not simulate the behavior of the member under realistic earthquake loading. Furthermore, the mode of failure in the columns is dependent on the boundary conditions which should reflect the total response of the structure.

In this study, earthquake behavior of steel box-section columns supporting a two-story frame structure are tested and verified using a substructured hybrid loading system. Inelastic response of the entire frame under severe earthquakes can be simulated using experimentally measured restoring forces of the critical first-story columns combined with analytical restoring forces of the rest of the structure.

2 SUBSTRUCTURED ON-LINE HYBRID LOADING TEST

During the last two decades, on-line hybrid test method (or pseudo-dynamic test method) has become a very powerful tool to test for inelastic earthquake response of structures. The original formulation of the on-line hybrid test involves fabrication of the complete structural prototypes for proper modeling. And yet, in most cases, severe inelastic deformations are likely to occur (as in the potential hinge regions in columns) only in certain localized regions.

By incorporating substructuring concepts into on-line hybrid test technique, a substructured on-line hybrid test method is developed in which only the critical regions are tested experimentally while the other 'well-behaved' regions of the structure are modeled analytically. As an example, the critical first-story columns of the two-story frame model (Fig. 1) are taken as the experimental substructures with the remaining members considered analytically. Thus, critical sub-assemblages and components can be tested economically under realistic load conditions considering proper boundary conditions. At the same time, inelastic earthquake response of the total structure can be reliably predicted.

The equations of motion of a nonlinear structural system may be expressed as follows:

$$[M]\{\ddot{u}\}_t + [C]\{\dot{u}\}_t + \{R_f\}_t = \{P\}_t \qquad (1)$$

in which $\{R_f\} = \{R_f\}^{\mathrm{MATH}} + \{R_f\}^{\mathrm{EXPT}}$

where $\{u\}_t$, $\{\dot{u}\}_t$, $\{\ddot{u}\}_t$: displacement, velocity, and acceleration vector at time t; $[M]$: mass matrix; $[C]$:

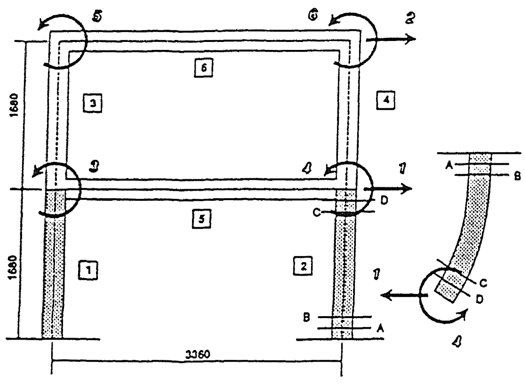

Fig. 1. Experimental and analytical substructures in a two-story frame model.

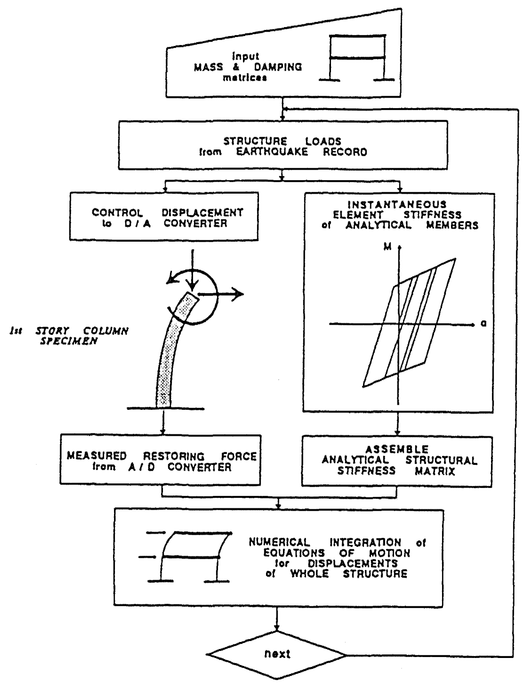

Fig. 2. Substructured hybrid loading test procedure.

viscous damping matrix; $\{R_f\}_t^{\mathrm{EXPT}}$: restoring forces to be measured experimentally from a specimen loaded based on its current deformation state; $\{R_f\}_t^{\mathrm{MATH}}$: restoring forces from analytical substructures characterized by mathematical models; and $\{P\}_t$: load vector at time t. Flowchart of the substructured hybrid loading test procedure is shown in Fig. 2.

2.1 Numerical Integration Schemes

Using the conditionally stable explicit integration method in substructured on-line hybrid tests of a MDOF system would necessitate extremely small integration time intervals in order to satisfy the required numerical stability criterion. This requirement is especially stringent in systems such as structural frame where the axial and rotation D.O.F.s are very much stiffer than the lateral ones. A class of so-called mixed integration methods originally developed for finite-element analysis of structure-fluid interaction has been found to be suitable for substructured hybrid tests (Nakashima et al. 1990; Dermitzakis and Mahin. 1985).

The OS method has been frequently used for substructured hybrid tests in Japan for the most recent tests based on the merits (Nakashima et al. 1990). It is adapted in the current implementation of this substructured hybrid loading test system used in the testing of steel box bridge piers presented here.

To implement the OS algorithm, Eqn. (1) is expressed as follows:

$$[M]\{\ddot{u}\}_{t+\Delta t} + [C]\{\dot{u}\}_{t+\Delta t} + \{R_f\}_{t+\Delta t}^{lnr} + \{R_f\}_{t+\Delta t}^{nonlnr} = \{P\}_{t+\Delta t}$$

$$[M]\{\ddot{u}\}_{t+\Delta t} + [C]\{\dot{u}\}_{t+\Delta t} + [K]\{u\}_{t+\Delta t} + (\{R_f\}_{t+\Delta t} - [K]\{\tilde{u}\}_{t+\Delta t}) = \{P\}_{t+\Delta t} \quad (2)$$

An explicit trapezoidal rule may be used for the predictive displacement vector as given by:

$$\{\tilde{u}\}_{t+\Delta t} = \{u\}_t + \Delta t\{\dot{u}\}_t + \left(\Delta t^2/4\right)\{\ddot{u}\}_t \quad (3)$$

On the other hand, an implicit trapezoidal rule (Newmark method with $\gamma = 0.5$ and $\beta = 0.25$) may be used:

$$\{u\}_{t+\Delta t} = \{\tilde{u}\}_{t+\Delta t} + \left(\Delta t^2/4\right)\{\ddot{u}\}_{t+\Delta t} \quad (4)$$

$$\{\dot{u}\}_{t+\Delta t} = \{\dot{u}\}_t + (\Delta t/2)\left(\{\ddot{u}\}_t + \{\ddot{u}\}_{t+\Delta t}\right) \quad (5)$$

The displacement and velocity expressions given above are substituted into Eqn. (2) to solve for the acceleration vector.

It has been shown (Plesha and Belytschko. 1985) that the OS integration method is unconditionally stable for materials with decreasing stiffness (hysteresis is of 'softening' type).

2.2 Three D.O.F. General In-plane Loading System

A 3-DOF general in-plane loading system capable of subjecting a specimen under combined axial, shear, and bending loads has been developed and implemented. The overall set-up of the test bed and test rig is shown in Fig. 3. One actuator is attached horizontally to the reaction wall, while two others are hanged vertically from the overhanging reaction girder. A rigid load-transfer beam was fabricated to transfer displacements and forces between the actuators and the specimen. Universal joints consisting of swivel heads and swivel bases are attached to both ends of each actuator.

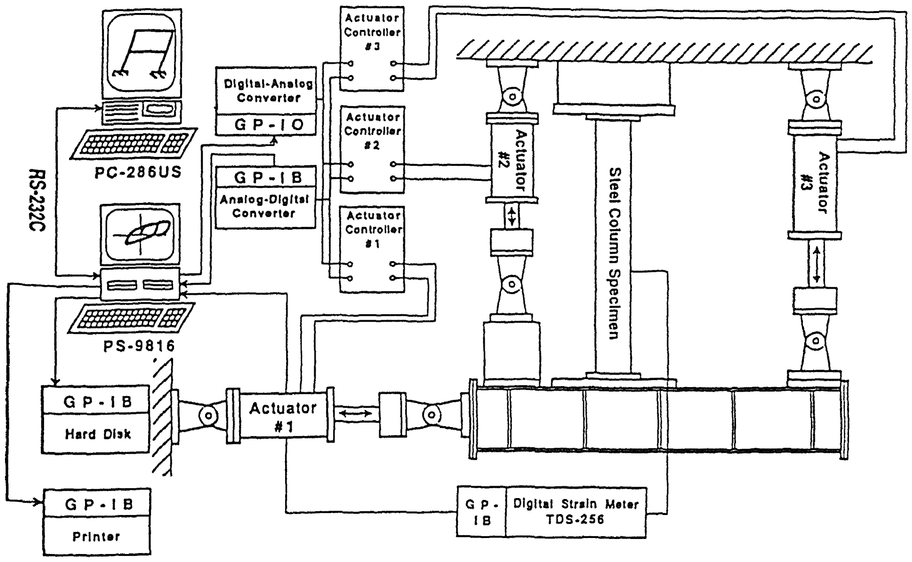

Fig. 3. Setup of loading and control system.

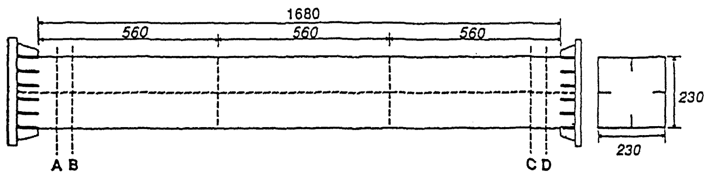

Fig. 4. Steel box-section column specimen.

Table 1. Sizes and dimensions.

SPECIMEN	REGION	SIZE (mm)
all	length	1680
	flange	230 by 3.2
	web	230 by 3.2
A and C	rib	27 by 4.5
B	rib	41 by 4.5

General displacement pattern of the experimental substructure are transformed into deformation of an equivalent cantilever model. For a desired deformation state in the cantilevered specimen tip defined by $\delta_x, \delta_y, \theta_z$, the restoring forces P_x, P_y, M_z are to be determined. The procedure is outlined in the following: (1). Initial lengths of the actuator pistons are computed at the initial set position with the specimen tip O taken as reference origin; (2). Compute constant distances and orientations within a rigid body between specimen tip O and the respective positions of the pivot hinge of the swivel heads; (3). For a desired deformation state defined by $[\delta_x, \delta_y, \theta_z]$, locate the new position of the pivot hinge of the respective swivel heads; (4). From the computed new positions of the swivel heads, compute the changes in lengths in order for the piston to reach these new positions; (5). Find the actuator displacement control signals $\Delta_1, \Delta_2, \Delta_3$ and send commands to D/A converter; (6). Load cells inside the actuators measure the forces induced in the pistons F_1, F_2, F_3 and readings taken by A/D converters; (7). Specimen restoring forces P_x, P_y, M_z are computed based on equilibrium equations of the rigid transfer beam; (8). And finally, cantilever restoring forces are transformed into the required restoring forces at the member ends.

3 TESTS OF STEEL BOX-SECTION COLUMNS FOR INELASTIC EARTHQUAKE RESPONSE OF FRAME STRUCTURES

3.1 Structural Models and Column Specimens

A two-story steel frame model (Fig. 1) is studied. The critical first-story columns are taken as the experimental substructures in which a specimen is loaded on-line to determine its restoring forces. The rest of the structure is modeled analytically using bilinear hysteretic models for simplicity in this study. Variation in ana-

Table 2. Outline of specimen types and loading cases.

specimen	no. of longitudinal stiffeners	no. of lateral stiffeners	τ/τ^*	σ_y	constant axial load (tonf)	constant moment (tonf-cm)	girder stiffness (col.stf.)	Remarks
A1	1	2	1	3000	17	0	—	Q.S. – single curvature
A2	1	2	1	3000	17	300	—	Q.S. – double curvature
A3	1	2	1	3000	17	—	1	S.H. – weaker girder
A4	1	2	1	3000	17	—	2	S.H. – stronger girder
B1	1	2	1	3000	18	0	—	Q.S. – single curvature
B2	1	2	1	3000	18	300	—	Q.S. – double curvature
B3	1	2	1	3000	18	—	1	S.H. – weaker girder
B4	1	2	1	3000	18	—	2	S.H. – stronger girder
C1	1	2	1	2000	11	0	—	Q.S. – single curvature
C2	1	2	1	2000	11	300	—	Q.S. – double curvature
C3	1	2	1	2000	11	—	1	S.H. – weaker girder
C4	1	2	1	2000	11	—	2	S.H. – stronger girder

Q.S. – quasi-static cyclic loading test; S.H. – substructured hybrid loading test

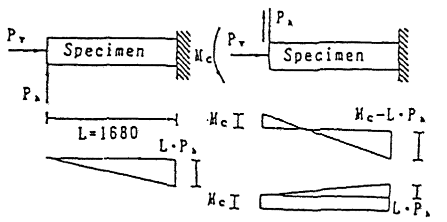

Fig. 5. Moment distribution pattern under QS loading.

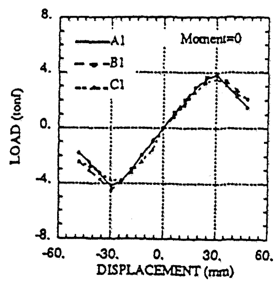

Fig. 6. Restoring forces envelopes.

lytical parameters include varying the level of yielding girders.

Specimens were fabricated corresponding to the full scale of the structural members being modeled. In this study, steel box-section column specimens were fabricated. The total length of the specimens is 1.680m. Three types of specimens were fabricated. The yield stress for the steel material used are: 3200 kg/cm^2 for Type A and Type B; and 2000 kg/cm^2 for Type C. Overall dimensions and stiffener configurations are summarized in Fig. 4 and Table 1.

3.2 Test Programs and Results

In addition to the main tests using substructured hybrid method, quasi-static cyclic loading tests were conducted. Unlike in the usual tests, a combined pattern of axial, shear, and bending loads can be imposed on the specimen tip. For each type of steel columns, four specimens were fabricated for four loading cases. Cases 1 and 2 are quasi-static cyclic loading tests, while cases 3 and 4 are substructured hybrid loading tests. Constant axial force equivalent to 16% of yield axial force is imposed on the specimens. The testing program is summarized in Table 2.

In Case 1 loading, cyclic lateral displacement with increasing amplitude is applied to the tip of the column specimen in addition to the constant axial load. In Case 2 loading, a constant bending moment equivalent to about 35% of the ultimate strength is imposed in addition to the constant axial load and increasing cyclic lateral displacements. Loading patterns of these two quasi-static cyclic loading cases are schematically illustrated in Fig. 5.

The envelopes of restoring moments under Case 1 loading for all the three types of steel columns are shown in Fig. 6. Although not much difference is observed between the different types of specimens, Type C specimen with lower yielding strength shows lower ultimate restoring force but with more ductile behavior in the inelastic range. To check on the effects of material strength on member behavior, moment-curvature relations of Types A and C at the section 10cm from the fixed end (Section A) are plotted in Fig. 7. Type A specimen shows higher ultimate resisting capacity than Type C, but deterioration in inelastic range is faster.

For lateral displacements producing moments in the same direction as the constant bending load, the spec-

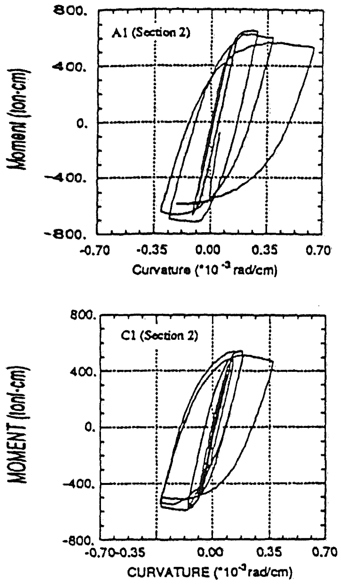

Fig. 7. Cyclic load-deformation behavior.

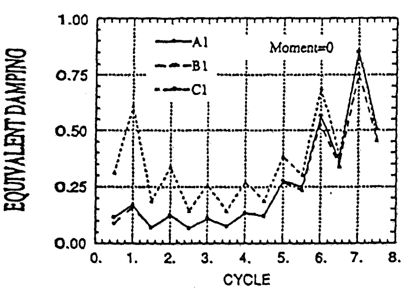

Fig. 8. Stiffness degradation under cyclic loads.

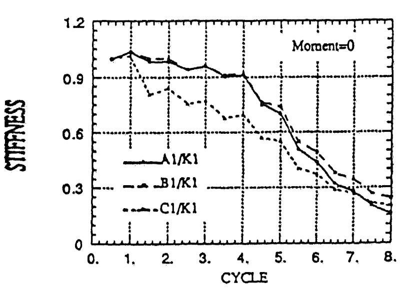

Fig. 9. Equivalent damping under cyclic loads.

imen deforms in single curvature under the moment distribution pattern shown in Fig. 5. Ultimate restoring forces in this direction for all the three types are lower than the ultimate strength observed under Case 1 loading.

For lateral displacements producing moments in the direction opposite to that of the applied constant bending loads, bending moment changes its sign along the member axis and the member deforms in double curvature. Higher ultimate strengths are observed compared to those under Case 1 loading. Among the different types, Type B specimen with the larger stiffeners shows the highest ultimate strength. Type C with the lower yielding steel and with normal amount of stiffeners show the lowest ultimate strength.

Equivalent damping and normalized stiffness are summarized for the tests under Case 1 loading as shown in Figs. 8 and 9. Under cycles of smaller displacements, Type C shows faster stiffness deterioration but higher values of equivalent damping than those of Types A and B. Under cycles of higher displacements, the normalized stiffness of Type B shows higher values than those of Types A and C. The equivalent damping tends to similar values for larger displacements.

After conducting the tests of isolated specimens under quasi-static loadings, substructured hybrid loading tests of the columns are conducted to determine its inelastic behavior and the interaction on the inelastic response of the total structure during earthquakes. The critical first-story columns of the frame model shown in Fig. 1 are taken as the experimental substructures. Loading cases 3 and 4 are substructured hybrid loading cases. In Case 3 loading, the girders are modeled to have the same stiffness as the columns. In Case 4 loading, the girders are modeled to have twice the stiffness of the columns. The fundamental natural period of the model is set at 0.7 sec. The El Centro NS record (1940) is used as the input earthquake ground motion.

Results of Type B specimens are presented in this paper. Time history response is given in Fig. 10. Fig. 10(a) shows the story displacements for Case 3 substructured hybrid loading of the column in the frame with more flexible girder, while Fig. 10(b) shows the story displacement response for Case 4 substructured hybrid loading test. Comparing (a) and (b), the upper story displacement is reduced due to stiffer structure (stiffer girders). The stiffer girders also reduced the rotation of the joints as shown in Fig. 10(c). Consequently, the first-story end of the tested column in Case 4 connected to a stiffer girder is displaced in a more constraining manner producing larger moment than in Case 3.

Maximum curvature distribution along the member axis is shown in Fig. 11. Large curvature response is observed near the fixed end (sections A and B) of the column in Case 3 frame. On the other hand, both ends of the columns in Case 4 frame undergo large curvatures due to the constraining effects of the stiffer girders. Moment-curvature response at the four sections are shown in Fig. 12 for Case 3 frame and in Fig. 13 for Case 4 frame. Large plastic behavior is clearly observed at sections A and D of Case 4 frame.

From the above results, it is observed that the girder stiffness has a large effect on the column behavior. Equally important, the consequent behavior of the columns greatly affects the overall response of the total structure. If the stiffness of the beam is smaller, interstory displacement will become large. on the other hand, if the girders are stiffer, displacements will be

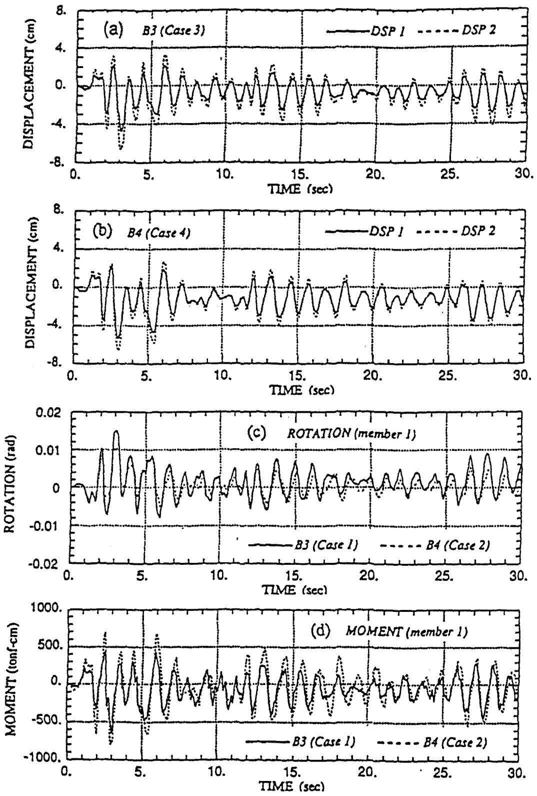

Fig. 10. Time histories of earthquake response.

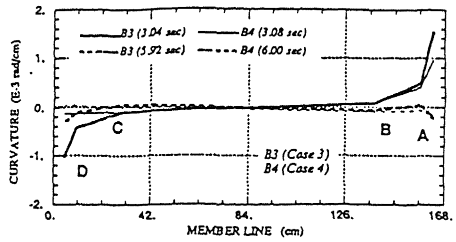

Fig. 11. Distribution of maximum curvatures.

smaller but plastic hinges may occur at both ends of the columns resulting in structural failure modes.

4 CONCLUDING REMARKS

Understanding the inelastic behavior of members and total structures is an essential approach to evaluate reliability of steel structures against possible strong ground motions. It is neccessary to verify the earthquake-resistant capacity of the critical column members by subjecting them to realistic earthquake loading.

In the experimental studies involved to achieve these, it is very important to be able to simulate inelastic behavior of members and structures under realistic earthquake loading conditions. In this paper, substructured hybrid loading system capable of subjecting a column specimen under realistic histories of combined axial, shear, and bending loads has been developed. Using this system, critical members can be tested under realistic earthquake loads and proper boundary conditions. Most importantly, inelastic earthquake response of the total structure can be reliably predicted.

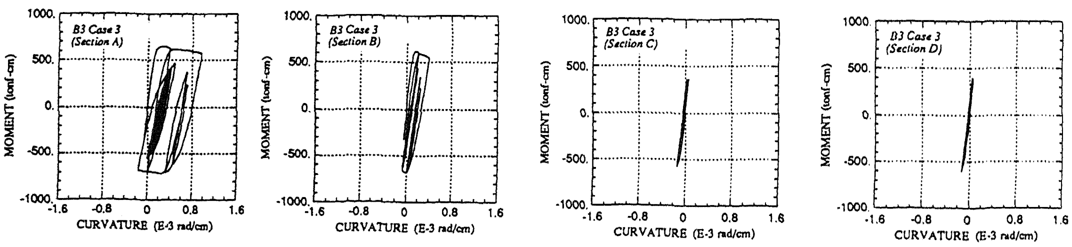

Fig. 12. Moment-curvature response for Type B3 under Case 3 substructured hybrid loading test.

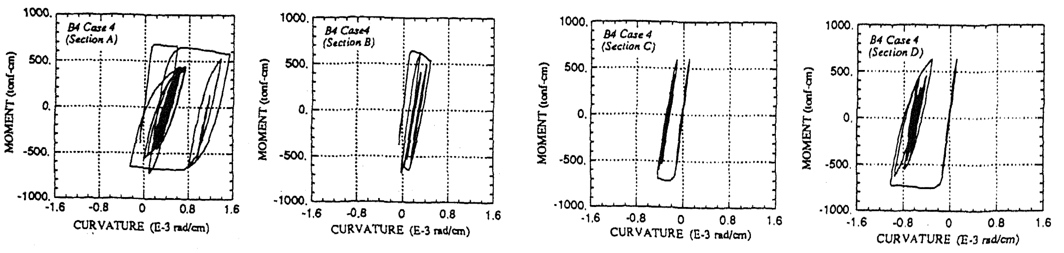

Fig. 13. Moment-curvature response for Type B4 under Case 4 substructured hybrid loading test.

ACKNOWLEDGEMENTS

The authors would like to acknowledge the cooperation of Mr. Kazuyuki Izùno (research associate) and Mr. Shinji Nakanishi (laboratory engineer) of Dept. of Civil Eng., Kyoto University throughout the experimental testing program. We would also like to express our thanks to Katayama Ironworks Co, for their assistance in fabricating the loading beam.

REFERENCES

Dermitzakis, S.N. and S.A. Mahin 1985.
Development of substructuring techniques for online computer controlled seismic performance testing. UCB/EERC-85/04. Earthquake Engineering Research Center, Univ. of California, Berkeley.

Nakashima, M., K. Ishii and K. Ando 1990.
Integration techniques for substructure pseudo dynamic test. Proceedings of 4th National Conference on Earthquake Engineering 2: 515–524.

Plesha, M. and T. Belytschko 1985.
A constitutive operator splitting method for nonlinear transient analysis. Computers and Structures. 20-4: 767–777.